

Persistent semi-metal-like nature of perovskite CaIrO_3 epitaxial thin films grown on different substrates

Abhijit Biswas, and Yoon Hee Jeong*

Department of Physics, POSTECH, Pohang, 790-784, South Korea

Abstract

We synthesized high quality *perovskite* (Pv) CaIrO_3 epitaxial thin films and made systematic study of resistivity within $300 \text{ K} \leq T \leq 10 \text{ K}$. Starting with the film on best lattice-matched substrate, we then altered underlying substrates imposing high tensile or compressive strain. The Pv- CaIrO_3 film on best lattice-matched substrate (on NdGaO_3 (110)) shows resistivity $\rho \sim 4 \text{ m}\Omega\cdot\text{cm}$ at 300 K. With decrease in temperature, we observed tiny increase in resistivity with $\rho \sim 5 \text{ m}\Omega\cdot\text{cm}$ at 10 K. $\rho(T)$ does not diverges at low T showing signature of semi-metal-like transport. Increasing tensile (compressive) strain on Pv- CaIrO_3 films (SrTiO_3 (001) and GdScO_3 (110) substrates for tensile strain and LaAlO_3 (001) and YAlO_3 (110) substrates for compressive strain) show decrease (increase) in resistivity, nevertheless, films remain semi-metal-like. Thus effective correlation is minutely modified and tensile (compressive) strain results in tiny increase (decrease) of electronic bandwidth. Moreover, magnetoresistance always remains positive with quadratic magnetic field dependence. This persistent semi-metal-like nature of Pv- CaIrO_3 thin films with minute changes in effective correlation by strain may provide new insights into strong spin-orbit coupled $5d$ based oxide physics.

PACS number(s): 71.20.Gj, 68.60.Bs, 84.37.+q, 68.55.-a

*Corresponding author: yhj@postech.ac.kr

Strong spin-orbit coupled $5d$ element based oxides are subject of recent investigations as it display many unique physical properties such as dimensionality controlled metal-insulator-transition (MIT), unconventional magnetic ordering, spin liquid behaviors, topological insulator characteristics.[1] In this regard, Ruddlesden-Popper series of strontium iridates, $\text{Sr}_{n+1}\text{Ir}_n\text{O}_{3n+1}$ ($n = 1, 2, \dots, \infty$) have been widely investigated, as increasing n , i.e. increasing the number of IrO_2 planes, changes its novel $J_{\text{eff}} = 1/2$ and $J_{\text{eff}} = 3/2$ band picture and systematic transition from insulator-to-metal have been observed because of interplay between local Coulomb interactions, strong spin-orbit coupling, dimensionality, and octahedral rotations.[2-4]

Recently analogous compound CaIrO_3 , attracts a lot attention due to its geophysical interest as the low dimensional *post-perovskite* (pPv) structure having space group- $Cmcm$, was found to similar of the archetype phase of the pPv polymorph of MgSiO_3 , found in Earth's D'' layer.[5,6] The pPv- CaIrO_3 is naively expected to be a good metal as it has iridium (Ir^{4+}) with extended $5d$ orbitals (wider band width) and t_{2g}^5 electron configuration; however, it actually exhibits Mott insulating $J_{\text{eff}} = 1/2$ state with resistivity $\rho \sim 10^4 \Omega\text{-cm}$ at room temperature. It also undergoes the canted antiferromagnetic phase transition at 115 K.[7-10] It has been concluded that strong spin-orbit coupling as well as Coulomb interactions play crucial role in resistivity and magnetization. In contrast, three dimensional *perovskite* (Pv) CaIrO_3 having space group- $Pbnm$ shows large drop of resistivity ($\sim 10^5$) with respect to pPv form, but still resistivity increases with decrease in temperature.[7] Surprisingly, resistivity does not diverges even at low temperature showing semi-metal-like nature, and the system also shows Pauli paramagnetic characteristics.[7] Although polycrystalline Pv- CaIrO_3 was shown to be of semi-metal-like and paramagnetic, but with

thin films however, one would take advantages over bulk ones because key parameters such as bandwidth (W), correlation (U) and the strength of spin-orbit coupling can be changed to some degree by varying lattice strains utilizing structurally compatible different lattice-mismatched substrates and thus Pv-CaIrO₃ thin films would also be able to provide new interesting phenomena, as similar in Pv- SrIrO₃ thin films.[11-13]

Recently, some efforts were given to synthesize Pv-CaIrO₃ thin films as this can only be stabilized at high pressure and temperature. Films were also found to be of semi-metal-like, and the system lies close to the MIT phase boundary.[14,15] As MIT in a correlated system is controlled by competition among relevant energy scales such as W , U , and spin-orbit coupling, the important parameters governing the physics are mainly the effective correlation (U/W), caused by a change in band width (W) by octahedral rotation.[14] As Pv-CaIrO₃ is a correlated system analogous to Pv-SrIrO₃, and lies close to the MIT phase boundary, so it is expected that applying strain in Pv-CaIrO₃ thin film would bring about corresponding changes in octahedral rotation and thus transport properties.

From thin films perspective, for Pv-ABO₃, bandwidth change as $W \propto \frac{\cos \varphi}{d^{3.5}}$, where d is the B-O bond length and $\varphi = (\pi - \theta)/2$ is the buckling deviation of the $B-O-B$ bond angle θ from π . An externally imposed strain by using various lattice miss-matched substrates would cause a change in band width as $B-O-B$ bond angle as well as bond length changes. It was often found that for Pv thin films, the in-plane strain is mostly adopted by tilting of BO₆ octahedra or a change in bond angle.[16-18] However, the relationship between the strain in the film and its bandwidth may not be so candid considering the biaxial nature of the strain in the film. Nevertheless, the average change in bond length and bond angle

would be sufficient in result of the corresponding change in bandwidth and therefore the transport properties.

In this report, we grew high quality epitaxial Pv-CaIrO₃ thin films and made systematic study of resistivity. Starting with film on best lattice matched substrate, we then altered the underlying substrates as these impose high tensile or compressive strain. Surprisingly, semi-metal-like nature in resistivity persists irrespective of imposed strain (tensile/compressive) with minute changes in resistivity. This persistent semi-metal-like characteristic implies that effective correlation (U/W) is minutely modified for Pv-CaIrO₃ thin films grown under different lattice-mismatched substrates.

We grew Pv-CaIrO₃ films by pulsed laser deposition (KrF laser with $\lambda = 248$ nm); ~ 40 nm thin films were grown on various lattice miss-matched substrates such as YAlO₃ (110), LaAlO₃ (001), NdGaO₃ (110), SrTiO₃ (001) and GdScO₃ (110). Pv-CaIrO₃ thin films were fabricated from a polycrystalline target made by mixing the stoichiometric amount of raw powders (CaCO₃ and IrO₂), pelletizing, and sintering at high temperature and ambient pressure. For growth the laser was operated at frequency 4 Hz, and the substrate temperature and oxygen partial pressure were 600 °C and 20 mTorr, respectively. All the films were post annealed at the same growth temperature and oxygen partial pressure for 30 min to compensate for any oxygen deficiency. It was noted that perovskite CaIrO₃ is of orthorhombic structure ($a = 5.35046$ Å, $b = 5.59291$ Å, $c = 7.67694$ Å)[19] and orthorhombic indices were typically used to indicate the orientation of orthorhombic substrates as in YAlO₃ (110), NdGaO₃ (110) and GdScO₃ (110). However, it was more convenient for mutual comparison to use *pseudocubic* and cubic lattice parameters with subscript 'c'. The pseudocubic (a_c) lattice parameter converted from the orthorhombic lattice parameters ($\sqrt{2} \times \sqrt{2} \times 2$) of bulk CaIrO₃ was found to be ~ 3.86 Å.[19,20] If one

takes this value literally, it would match NdGaO₃ substrate ($a_c = 3.86 \text{ \AA}$) and correspond to +3.76%, and +1.85% compressive strain for the films on YAlO₃ ($a_c = 3.72 \text{ \AA}$), and LaAlO₃ substrates ($a_c = 3.86 \text{ \AA}$); -1.15%, and -2.52% tensile strain for the films on SrTiO₃ ($a_c = 3.905 \text{ \AA}$), and GdScO₃ substrates ($a_c = 3.96 \text{ \AA}$), respectively. The in-plane lattice parameter of the substrates in relationship to that of Pv-CaIrO₃ (Fig. 1); it was seen that the substrates range conveniently from very well matched (NdGaO₃) to strongly mismatched (GdScO₃ and YAlO₃).

X-ray diffraction (XRD) measurements (θ - 2θ scan) of the Pv-CaIrO₃ films synthesized as described above show the crystalline (001)_C peak without any impurity or additional peaks; for clarity, only the low angle data was shown (Fig. 2a). Films on all the substrates (except on LaAlO₃) display thickness fringes confirming high crystalline quality. In case of film on LaAlO₃ substrate, the dense twinning of substrate was probably responsible for degrading the surface quality. To confirm more about sample quality, we took the perfect lattice-matched film (on NdGaO₃) and further characterize the crystallinity. Reflectivity showing nice oscillations (Fig. 2b) as well as ω scans (rocking curve) were performed (Fig. 2c). For rocking curve analysis around the (001)_C peak of Pv-CaIrO₃ films, the center positions of full width at half maximum (FWHM) coincided and made to zero value. FWHM was found to be small ($\sim 0.032^\circ$). We had also measured the strain in the CaIrO₃ films grown especially on the GdScO₃ and YAlO₃ substrates (highest lattice miss-match on both ends) utilizing reciprocal space mapping (RSM). The RSM results around the inplane (103)_C reflection peak of the Pv-CaIrO₃ film were shown (Fig. 1d and 1e). Film on GdScO₃ substrate (-2.52% tensile strain) was almost fully strained, [14] whereas film on YAlO₃ substrate (+3.76% compressive strain) was relaxed. It's a common possibility for thin films because highly-strained epitaxial films try to relax to minimize the accumulating strain energy, and these

increases with the lattice-mismatch. Having characterized the structural quality of films, next electrical transport measurements were performed using the four-probe van der Pauw geometry within $300 \text{ K} \leq T \leq 10 \text{ K}$.

Measured electrical resistivities of Pv-CaIrO₃ films grown on various lattice-mismatched substrates were shown within the temperature range of $300 \text{ K} \leq T \leq 10 \text{ K}$ (Fig. 3). Film on best lattice-matched substrate (on NdGaO₃) shows room temperature resistivity (ρ) $\sim 4 \text{ m}\Omega\cdot\text{cm}$, which was much smaller than bulk polycrystalline Pv-CaIrO₃ ($\rho \sim 100 \text{ m}\Omega\cdot\text{cm}$ at 300 K) [7]; this fact can be understood by noting that the measured resistivity in bulk polycrystals were affected by large grain boundaries and porosity. Tiny increase in resistivity with the decrease in temperature was observed down to 10 K. Surprisingly, resistivity ($\rho(T)$) did not diverged even at low T (also change in resistivity $\frac{\rho_{300\text{K}}}{\rho_{10\text{K}}}$ was found to be very small); a signature of semi-metal-like characteristics.[14] Increasing the *tensile* strain on film (on SrTiO₃) reduces the room temperature resistivity. Imposing more tensile strain on film (on GdScO₃) further decreases the resistivity with $\rho \sim 3 \text{ m}\Omega\cdot\text{cm}$ at room temperature. But the overall resistivity features within the temperature range of $300 \text{ K} \leq T \leq 10 \text{ K}$ were as similar as film on best lattice-matched substrate; these films were also semi-metal-like. Imposing *compressive* strain, by growing films (on LaAlO₃) and then more compressive one (on YAlO₃) show increase in resistivity with respect to best lattice-matched film as $\rho \sim 6 \text{ m}\Omega\cdot\text{cm}$ at room temperature. Even in this situation resistivity nature remains to be semi-metal-like as $\rho(T)$ did not diverged at low T . This definitely makes implications that however small the effect was, effective correlation (U/W) modified the gap between lower Hubbard band (*LHB*) and upper Hubbard band (*UHB*) as strain had an impact on the Ir-O-Ir bond angle and Ir-O bond length and thus change in bandwidth (W).[17]

Comparisons of electrical resistivity of Pv-SrIrO₃ and Pv-CaIrO₃ on respective best lattice-matched substrates were shown (Fig. 4). Pv-SrIrO₃ film (on GdScO₃) remains fully metallic (decreases in resistivity with the decrease in temperature) in whole temperature range ($300 \text{ K} \leq T \leq 10 \text{ K}$). In contrast, resistivity of Pv-CaIrO₃ thin film (on NdGaO₃) increases with the decrease in temperature but $\rho(T)$ did not diverged even at low T . Hall effect measurement confirm more about semi-metal-like behavior as the carrier concentration (n) was found $\approx 10^{20} \text{ cm}^{-3}$ at 300 K; characteristics of a semi-metal. The resistivity of Pv-CaIrO₃ was also found to be five times higher than of Pv-SrIrO₃ at low temperature. Even at room temperature, resistivity was found to be of $\sim 1.5 \text{ m}\Omega\cdot\text{cm}$ for Pv-SrIrO₃ [11], and $\sim 4 \text{ m}\Omega\cdot\text{cm}$ for Pv-CaIrO₃. This confirms that even in this semi-metal-like picture, effective correlation (U/W) affects bandwidth as the ionic radii is small for Ca²⁺ than Sr²⁺ (0.99 Å for Ca²⁺ and 1.13 Å for Sr²⁺), which changes the $B-O-B$ both length and bond angle. The correlation effect was then enhanced for Pv-CaIrO₃ with respect to Pv-SrIrO₃ which reduces the band width (W). In future it would be desirable to make direct observation of ARPES spectra; similar to Pv-SrIrO₃ to quantitatively verify the band picture of Pv-CaIrO₃ thin film[4], as well as the phase diagram of Pv-CaIrO₃ by tuning the interaction and spin-orbit coupling, as similar in SrIrO₃. [21]

Magnetoresistance (MR), change of resistivity of a material due to applied magnetic field (B) is an interesting phenomenon in high spin-orbit coupled systems. Also measurement of MR occasionally gives the indication about magnetic ordering, as for magnetically ordered systems MR was found negative. We measured MR of films on GdScO₃ and YAlO₃ substrates; highly tensile one as well as highly compressive one, with an applied magnetic field up to $\pm 9 \text{ T}$ along out-of-plane configuration at $T = 10 \text{ K}$. In both cases, we observed positive MR (Fig. 5) and $\propto B^2$. This positive MR in both cases may be attributed to the

Lorentz contribution.[11] This positive MR also indicates that the low temperature unusual behavior in resistivity (shoulder at low T ; Fig. 3) may not be associated with any kind of long-range magnetic ordering. This had further been confirmed with magnetization measurements (not shown here) which show that system remains to be paramagnetic (as similar in polycrystalline Pv-CaIrO₃ [7]). As magnetic moment was found to be very low (as expected for a system containing $5d$ element having weak correlation) and close to noise level, conclusive evidence about magnetism in Pv-CaIrO₃ thin film needs further investigation on microscopic level.

In summary, we grew high quality epitaxial Pv-CaIrO₃ thin films on various lattice-mismatched substrates by pulsed laser deposition. Resistivity measurement on best lattice-matched substrate shows that film was semi-metal-like. This semi-metal-like resistivity persists even by applying large tensile or compressive strain on films, by using lattice-mismatched substrates; thus making minute modification to effective correlation. Moreover films show positive MR with quadratic magnetic field dependence. This persistent semi-metal-like nature with tiny modification of effective correlation by strain may provide new insights for strong spin-orbit coupled $5d$ based oxide physics.

We would like to thank Y. -W. Lee and S. -W. Kim for technical helps. Authors would also like to thank KBSI Daegu for RSM measurements. This work was supported by the National Research Foundation via SRC at POSTECH (2011-0030786).

References

1. W. W. -Krempa, G. Chen, Y.-B. Kim, and L. Balents, *Condens. Matter Phys.* **5**, 2014 (2013). ([10.1146/annurev-conmatphys-020911-125138](https://doi.org/10.1146/annurev-conmatphys-020911-125138))
2. B. J. Kim, H. Ohsumi, T. Komesu, S. Sakai, T. Morita, H. Takagi, and T. Arima, *Science* **323**, 1329 (2009). ([10.1126/science.1167106](https://doi.org/10.1126/science.1167106))
3. S. J. Moon, H. Jin, K. W. Kim, W. S. Choi, Y. S. Lee, J. Yu, G. Cao, A. Sumi, H. Funakubo, C. Bernhard, and T. W. Noh, *Phys. Rev. Lett.* **101**, 226402 (2008). (<http://dx.doi.org/10.1103/PhysRevLett.101.226402>)
4. Y. F. Nie, P. D. C. King, C. H. Kim, M. Uchida, H. I. Wei, B. D. Faeth, J. P. Ruf, J. P. C. Ruff, L. Xie, X. Pan, C. J. Fennie, D. G. Schlom, and K. M. Shen, *Phys. Rev. Lett.* **114**, 016401 (2015). (<http://dx.doi.org/10.1103/PhysRevLett.114.016401>)
5. M. Murakami, K. Hirose, K. Kawamura, N. Sata, Y. Ohishi, *Science* **304**, 855 (2004). ([10.1126/science.1095932](https://doi.org/10.1126/science.1095932))
6. K. Hirose and Y. Fujita, *Geophys. Res. Lett.* **32**, L13313 (2005). ([10.1029/2005GL023219](https://doi.org/10.1029/2005GL023219))
7. K. Ohgushi, T. Yagi, H. Gotou, Y. Kiuchi, Y. Ueda, *Physica B* **404**, 3261 (2009). ([10.1016/j.physb.2009.07.084](https://doi.org/10.1016/j.physb.2009.07.084))
8. K. Ohgushi, J. Yamaura, H. Ohsumi, K. Sugimoto, S. Takeshita, A. Tokuda, H. Takagi, M. Takata, and T. Arima, *Phys. Rev. Lett.* **110**, 217212 (2013). (<http://dx.doi.org/10.1103/PhysRevLett.110.217212>)
9. M. M. Sala, K. Ohgushi, A. Al-Zein, Y. Hirata, G. Monaco, and M. Krisch, *Phys. Rev. Lett.* **112**, 176402 (2014). (<http://dx.doi.org/10.1103/PhysRevLett.112.176402>)
10. N. A. Bogdanov, V. M. Katukuri, H. Stoll, J. van den Brink, L. Hozoi, *Phys. Rev. B* **85**, 235147 (2012).

- <http://dx.doi.org/10.1103/PhysRevB.85.235147>)
11. A. Biswas, K. -S. Kim, and Y. H. Jeong, *J. Appl. Phys.* **116**, 213704 (2014).
<http://dx.doi.org/10.1063/1.4903314>)
 12. J. H. Gruenewald, J. Nichols, J. Terzic, G. Cao, J. W. Brill and S. S.A. Seo,
J. Mater. Res. **29**, 2491 (2014). (<http://dx.doi.org/10.1557/jmr.2014.288>)
 13. L. Zhang, Q. Liang, Y. Xiong, B. Zhang, L. Gao, H. Li, Y. B. Chen, J. Zhou, S.-T. Zhang, Z.-B. Gu, S. Yao, Z. Wang, Y. Lin, Y.- F. Chen, *Phys. Rev. B* **91**,035110 (2015).
<http://dx.doi.org/10.1103/PhysRevB.91.035110>)
 14. S. Y. Jang, H. Kim, S. J. Moon, W. S. Choi, B. C. Jeon, J. Yu and T. W. Noh, *J. Phys.:*
Condens. Matter **22**, 485602 (2010). ([doi:10.1088/0953-8984/22/48/485602](https://doi.org/10.1088/0953-8984/22/48/485602))
 15. D. Hirai, J. Matsuno, H. Takagi, arXiv:1501.01433.
 16. J. M. Rondinelli and N. A. Spaldin, *Adv. Mater.* **23**, 3363 (2011).
[10.1002/adma.201101152](https://doi.org/10.1002/adma.201101152))
 17. J. Nichols, J. Terzic, E. G. Bittle, O. B. Korneta, L. E. De Long, J. W. Brill, G. Cao,
and S. S. A. Seo, *Appl. Phys. Lett.* **102**, 141908 (2013).
<http://dx.doi.org/10.1063/1.4801877>)
 18. R. Aso, D. Kan, Y. Shimakawa and H. Kurata, *Sci. Rep.* **3**, 2214 (2013)
[10.1038/srep02214](https://doi.org/10.1038/srep02214))
 19. J. -G. Cheng, J. -S. Zhou, J. B. Goodenough, Y. Sui, Y. Ren, and M. R. Suchomel,
Phys. Rev. B **83**, 066401 (2011). (<http://dx.doi.org/10.1103/PhysRevB.83.064401>)
 20. N. Keawprak, R. Tu and T. Goto, *J. Ceram. Soc. Jpn.* **117**, 466 (2009).
<http://dx.doi.org/10.2109/jcersj2.117.466>)
 21. M. A. Zeb and H. -Y. Kee, *Phys. Rev. B* **86**, 085149 (2012).
<http://dx.doi.org/10.1103/PhysRevB.86.085149>)

Figure Captions

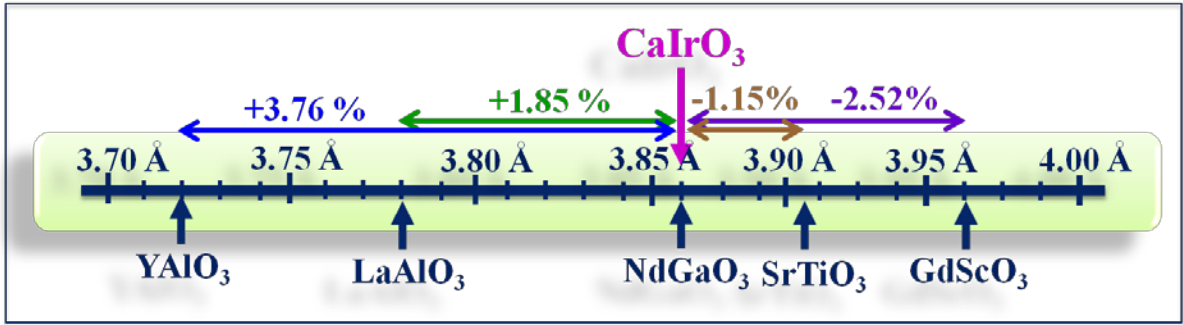
FIG. 1. (Color Online) Pseudo-cubic (or cubic) lattice constants of Pv-CaIrO₃ and used substrates: YAlO₃ (110), LaAlO₃ (001), NdGaO₃ (110), SrTiO₃ (001) and GdScO₃ (110). Corresponding amount of strain were also shown; tensile (–ve) and compressive (+ve).

FIG. 2. (Color Online) X-ray θ - 2θ scan of Pv-CaIrO₃ thin films grown on different substrates. Only low angle pseudo cubic (001)_C peaks were shown for clarity. Thickness fringes were clearly visible indicating high crystalline quality. (b)-(c) Reflectivity and full width half maxima (FWHM) of film grown on best lattice-matched substrate (on NdGaO₃) were shown. (d)-(e) Reciprocal space mapping (RSM) of films on high lattice-mismatched substrates were also shown. While film on GdScO₃ (110) was almost fully strained but relaxed nature was observed for film on YAlO₃ (110).

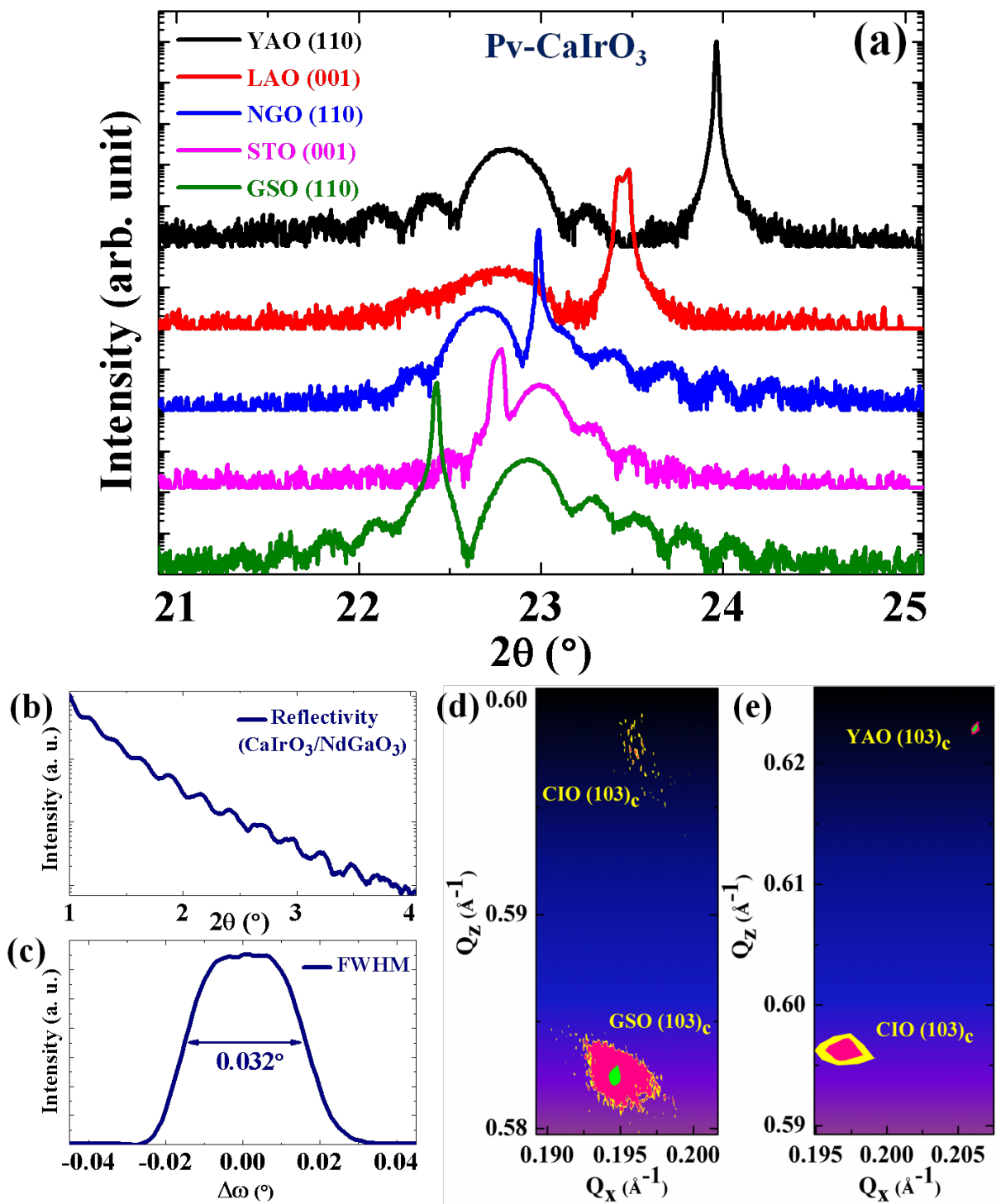
FIG. 3. (Color Online) Temperature dependence of the electrical resistivity (ρ) of Pv-CaIrO₃ films grown on different substrates. In all cases ρ (T) did not diverged even at low T , indicating the semi-metal-like characteristics of Pv-CaIrO₃ films.

FIG. 4. (Color Online) Comparison of electrical resistivity of Pv-CaIrO₃ and Pv-SrIrO₃ thin films grown on respective best lattice-matched substrates (CaIrO₃, NdGaO₃: $a_c \sim 3.86$ Å and SrIrO₃, GdScO₃: $a_c \sim 3.96$ Å).

FIG. 5. (Color Online) Positive magnetoresistance ($\propto B^2$) measured for Pv-CaIrO₃ films (on GdScO₃ and YAlO₃) at $T = 10$ K, with magnetic field strength upto ± 9 T along out-of-plane configuration.



(Figure--1)



(Figure--2)

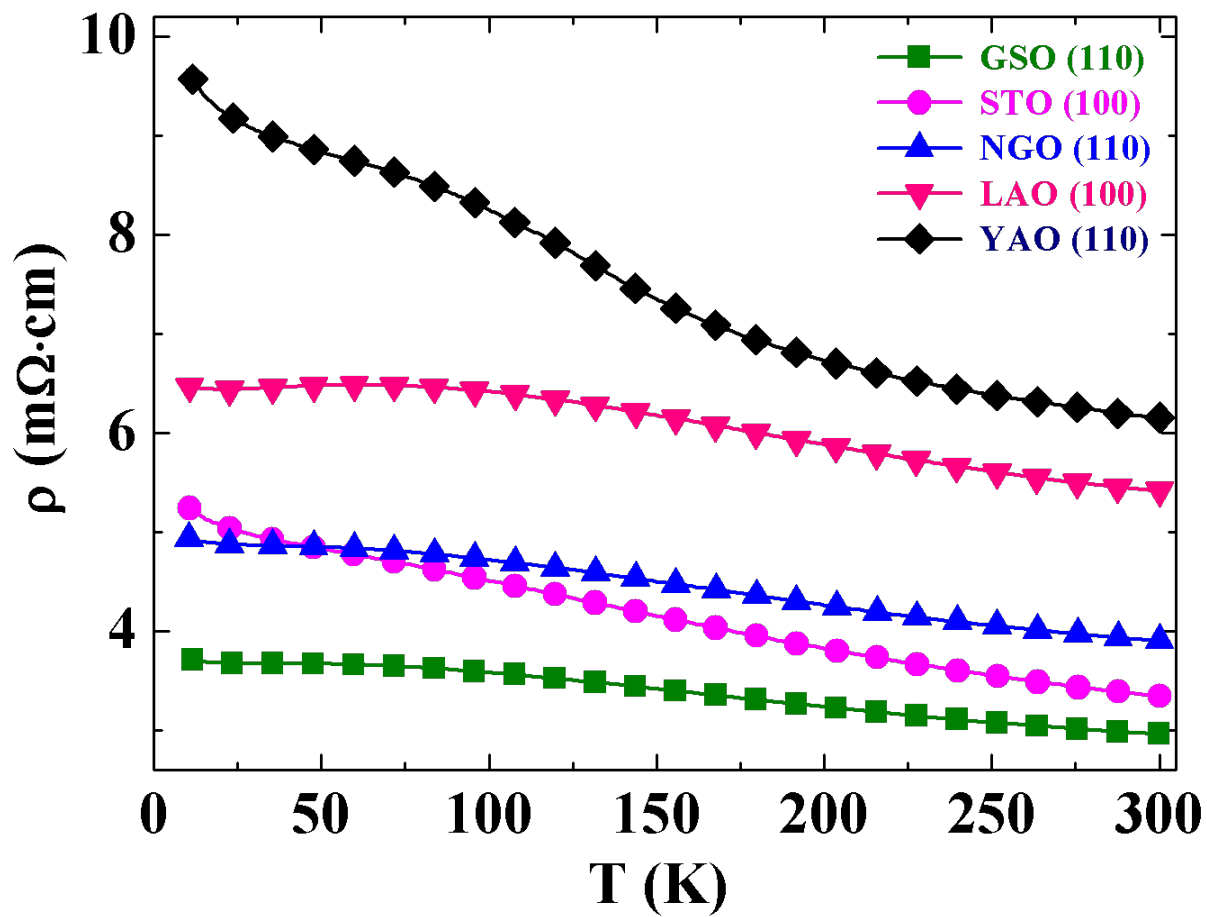


(Figure--3)

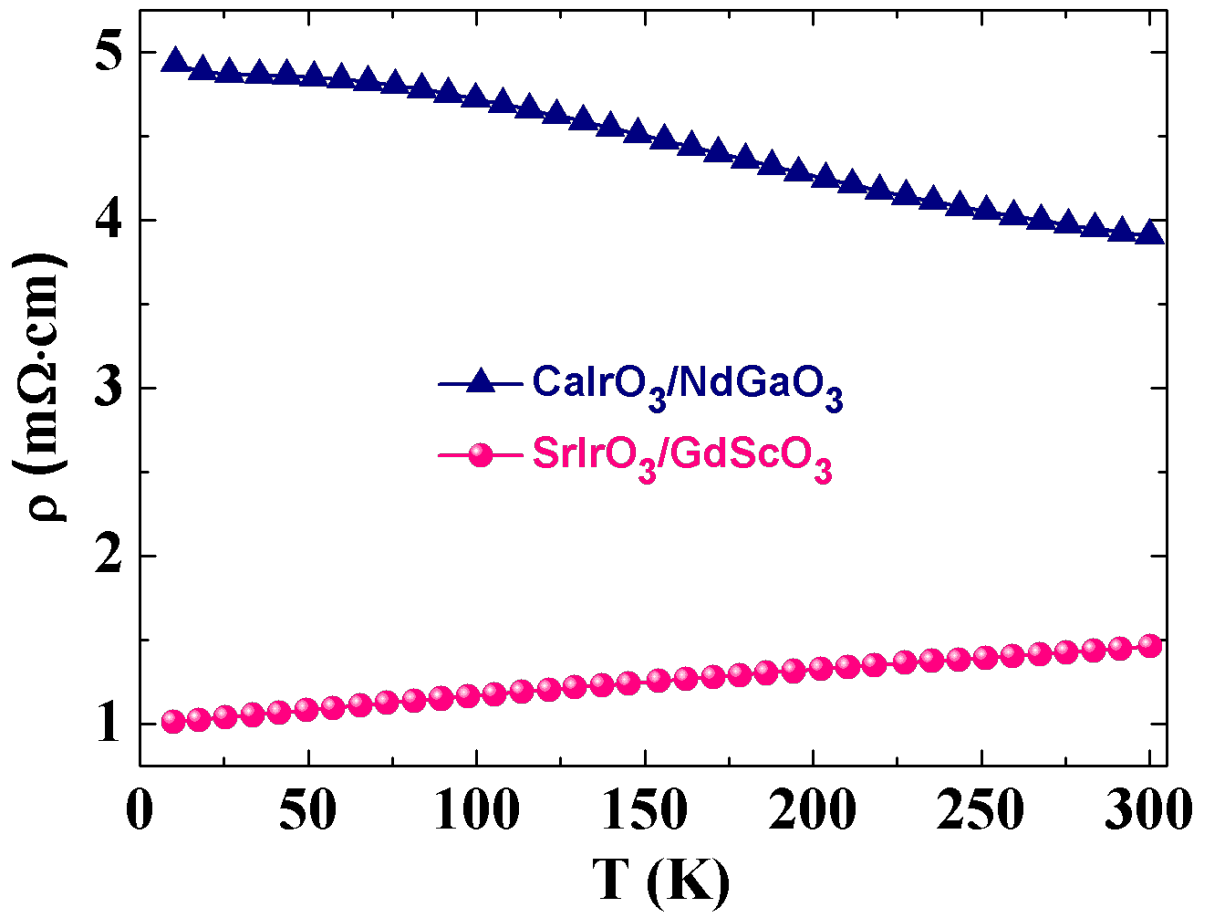


(Figure--4)

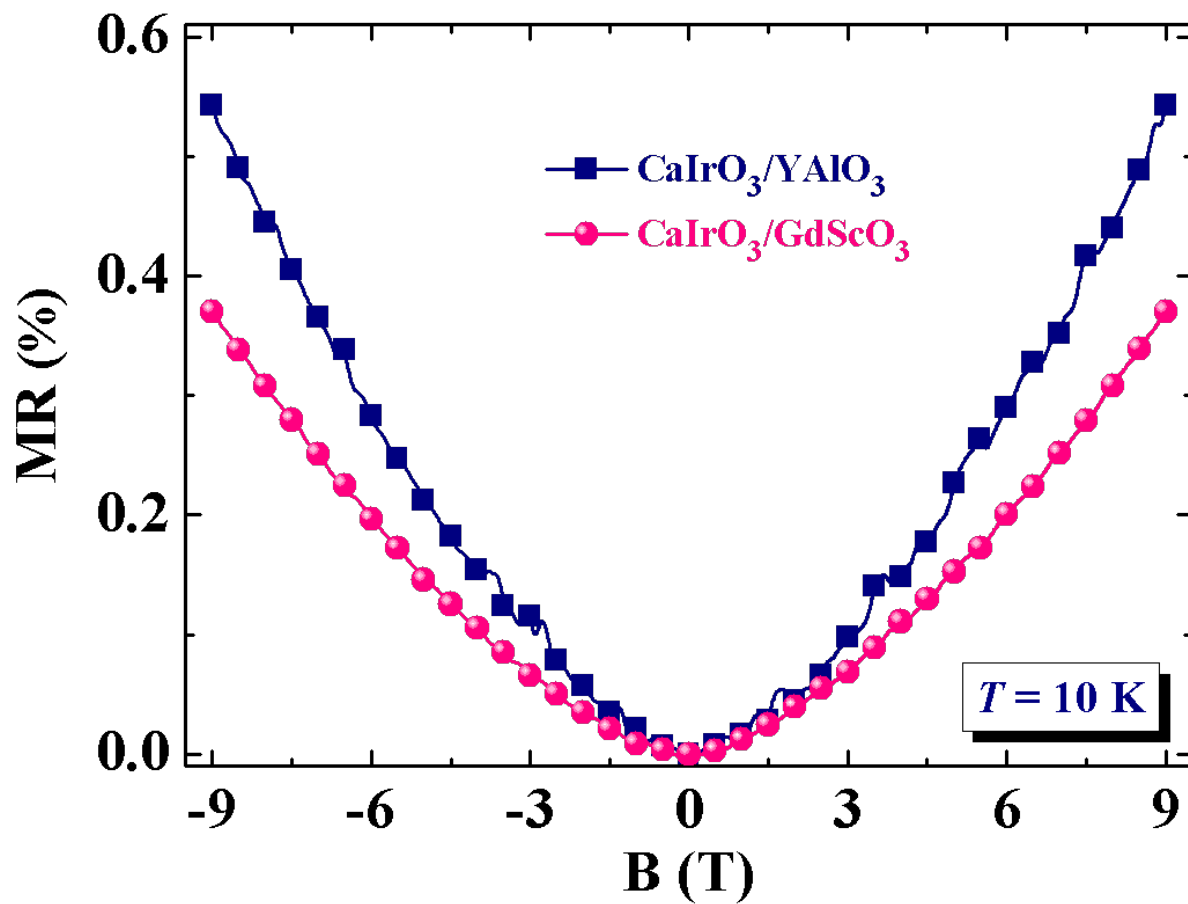


(Figure--5)